Switching of 800 nm femtosecond laser pulses using a compact PMN-PT modulator

Peter Adany,[1] E. Shane Price,[2] Carey K. Johnson,[2] Run Zhang,[3] and Rongqing Hui[1]
[1]*Department of Electrical Engineering & Computer Science, University of Kansas, Lawrence, Kansas 66045, USA*
[2]*Department of Chemistry, University of Kansas, Lawrence, Kansas 66045, USA*
[3]*Boston Applied Technologies, Inc., 6F Gill Street, Woburn, Massachusetts 01801, USA*

(Received 14 November 2008; accepted 11 February 2009; published online 13 March 2009)

A voltage-controlled birefringent cell based on ceramic PMN-PT material is used to enable fast intensity modulation of femtosecond laser pulses in the 800 nm wavelength window. The birefringent cell based on a PMN-PT compound has comparatively high electro-optic response, allowing for a short interaction length of 3 mm and thus very small size, low attenuation of 0.16 dB, and negligible broadening for 100 fs optical pulses. As an application example, agile wavelength tuning of optical pulses is demonstrated using the soliton self-frequency shift in a photonic crystal fiber. By dynamically controlling the optical power into the fiber, this system switches the wavelength of 100 fs pulses from 900 nm to beyond 1120 nm with less than 5 μs time. In addition, a feedback system stabilizes the wavelength drift against external conditions resulting in high wavelength stability. © *2009 American Institute of Physics.* [DOI: 10.1063/1.3093811]

I. INTRODUCTION

Femtosecond pulsed lasers in the near-IR wavelength range are highly useful for imaging live tissues and cells with common fluorescent markers. The extremely high peak power causes multiphoton absorption, producing a reduced focal volume for improved resolution. Combined with the low absorption of biological materials at the pump wavelength, this imaging technique minimizes cellular damage and autofluorescent background while improving image contrast.

Fast adjustment of both output optical power and emission wavelength are desirable for many applications including two-photon microscopy,[1,2] multiphoton precision microfabrication,[3] optical storage, and nonlinear optical signal processing. Wavelength tuning is useful for selective excitation of fluorescent dyes or reagents, and rapid wavelength switching can capture the dynamics of chemical reactions in living specimens.

Passively mode-locked Ti:Sapphire lasers can be used to generate pulses at 800 nm wavelength with $<$100 fs pulse width. More recently, compact and stable fiber-based femtosecond lasers have also been developed, which simplify many practical applications. However, high speed intensity modulation of femtosecond optical pulses in the near-infrared wavelength window has been challenging. In addition to minimizing power attenuation, chromatic dispersion has to be kept very small in order not to cause significant broadening of the laser pulse. One method to modulate the intensity of femtosecond laser output is by the use of an acousto-optic modulator (AOM). However, due to the dispersive nature of the diffracted beam in an AOM, significant broadening is expected at the 800 nm pump wavelength for short optical pulses. It is possible to compensate for this effect using a paired-AOM configuration, in which the special alignment of two AOMs cancels the pulse broadening caused by each AOM.[4] However, this solution apparently requires mechanical alignment and additional optical components, and therefore the system becomes rather complicated.

Another widely known intensity modulation setup uses a polarization retarder followed by a fixed polarizer. Unfortunately, many electrically controlled materials operating in the near-IR wavelength window typically have either high attenuation or low polarization-modulation efficiency. potassium dihydrogen orthophosphate (KDP)-based Pockels cells are typically bulky and require kilovolt levels of driving voltage (V_π) to achieve $\pi/2$ polarization rotation. From a practical application point of view, there is clearly a need for a high-speed and miniature intensity modulator for femtosecond optical pulses in near-IR wavelength region. In this paper, we demonstrate the use of a PMN-PT polarization retarder to construct an intensity modulator for femtosecond optical pulses, which has $>$95% transmission, negligible chromatic dispersion in the near-IR window, and a microsecond switching speed that is mainly limited by the voltage driver circuit and capacitance of the rotator element. We also demonstrate that fast wavelength modulation can be achieved by incorporating this intensity modulator in a soliton self-frequency shifter (SSFS) based on a nonlinear fiber.

II. CERAMIC-BASED ELECTRO-OPTIC INTENSITY MODULATOR

The polarization retarder is the key component in the polarizer-based intensity modulator. The material birefringence increases in response to an externally applied electrical potential, thus altering the exit polarization. A number of materials have been used for this purpose including KDP, $LiNbO_3$, liquid crystals, PLZT, and PMN-PT. Among these, PMN-PT has several notable advantages, such as a high

 © 2009 American Institute of Physics

This article is copyrighted as indicated in the article. Reuse of AIP content is subject to the terms at: http://scitationnew.aip.org/termsconditions. Downloaded to IP: 129.237.46.100 On: Tue, 16 Sep 2014 13:59:45

electro-optic (EO) coefficient, low hysteresis, a fast EO response, and low scattering loss for operation in the near-IR wavelength region.[5,6] The highest linear EO coefficient of PMN-PT is 2.8×10^{-15} m^2/V^2, which enables the construction of polarization modulators with short interaction length and low driving voltage. For example, for a PMN-PY based retarder with 3 mm optical length and 3.5 mm width, the V_π value is approximately 275 V. As a comparison, the V_π of a $LiNbO_3$-based retarder of the same size would be approximately 8000 V. In addition, since the material is composed of polycrystalline ceramic granules, it is isotropic with respect to the orientation of the applied electrical field, and therefore no birefringence is introduced when the external bias voltage is removed.

PMN-PT are a family of transparent, naturally durable, oxide EO ceramic materials. Their crystallographic structure is perovskite type with the formulation of ABO_3. The typical representatives of this family are $Pb_{1-x}La_x(Zr_yTi_{1-y})_{1-x/4}O_3$ (PLZT), $Pb(Mg_{1/3}Nb_{2/3})O_3-PbTiO_3$ (PMN-PT), and $Pb(Zn_{1/3}Nb_{2/3})O_3-PbTiO_3$ (PZN-PT). The PLZT formula assumes that La^{3+} substitutes for Pb^{2+} in the *A*-site and the *B*-site vacancies are created for electrical balance. The PLZT composition is conventionally abbreviated as $x/y/1-y$, by which a PLZT 9/65/35 composition means a La^{3+} concentration of 9% with a Zr/Ti ratio of 65 to 35. To achieve best transparency and EO coefficient, some elements, such as Ba and/or La, are usually added to the solid solutions of PMN-PT and PZN-PT.

Ferroelectric ceramics are traditionally made from powders formulated from individual oxides; however, for EO materials powders made from a chemical coprecipitation technique are more appropriate. This is because optical properties are highly sensitive to inhomogeneities, and understandably the EO ceramics require a higher purity, more homogeneous, and high-reactivity powder than other nonoptic materials.

For the polarization modulator, the thickness of the PMN-PT optoceramic element was 3 mm, and both surfaces were antireflection coated to minimize Fresnel reflections. The measured attenuation for an 800 nm optical signal passing through the polarization modulator was approximately 0.16 dB, or equivalently 96% transmission. For application as an intensity modulator, the PMN-PT cell was followed by a fixed polarizer and therefore the voltage-induced birefringence change resulted in the change of power transmission efficiency. Figure 1(a) shows the measured transmission efficiency of the device as the function of the applied bias voltage. Maximum power attenuation occurs at a 275 V bias, implying that V_π=275 V for the full range of phase modulation.

The dynamic response of the modulator when driven by a square wave voltage is shown in Fig. 1(b), where the 10%–90% switch-off time of the transmission is approximately 3 μs, which was mainly limited by the driver electrical circuit. Since the electrical capacitance of the optoceramic polarization modulator is approximately 680 pF, a submicrosecond switching speed is feasible with an improved driver circuit design. The optical source for the measurement was an 800 nm fiber laser with 110 fs pulse width and 70 MHz repetition rate (Femtolite F-100, IMRA Inc.). Results in Fig. 1 were measured with a photodiode with 100 MHz bandwidth, so that the individual optical pulses were not distinguishable. In order to evaluate the pulse broadening introduced by the intensity modulator, an autocorrelator was used to measure the width of each individual optical pulse at the modulator output, which tends out to be about 111 fs. This pulse width is practically the same as that of the fiber laser, which is 110 fs. Therefore, the effect of pulse broadening due to the intensity modulator is negligible.

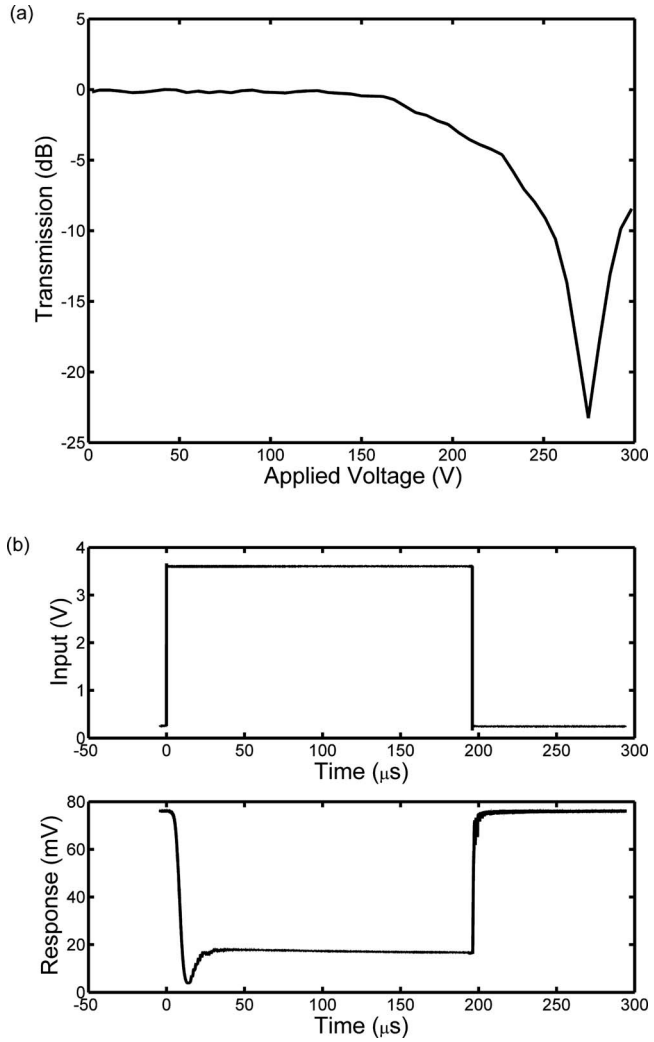

FIG. 1. Transmission vs applied voltage (a) and time-domain response of intensity modulation (b) for the PMN-PT optoceramic element.

In polarization modulators based on the linear EO effect, pulse broadening is mainly caused by chromatic dispersion, which is determined by the wavelength-dependent refractive index of the material itself. For modulating ultrashort optical pulses, it is important to evaluate the dispersion effect of the material. Figure 2(a) shows the refractive index of the PMN-PT measured by an ellipsometer. The chromatic dispersion coefficient, which indicates the differential group delay of the optical signal over a unit wavelength interval and a unit propagation length, can be calculated as $D=-(\lambda/c)\times[d^2n(\lambda)/d\lambda^2]$, where n is the wavelength-dependent refractive index, λ is the wavelength, and c is the speed of light, and the result is graphed in Fig. 2(b) as the solid line. As an

This article is copyrighted as indicated in the article. Reuse of AIP content is subject to the terms at: http://scitationnew.aip.org/termsconditions. Downloaded to IP: 129.237.46.100 On: Tue, 16 Sep 2014 13:59:45

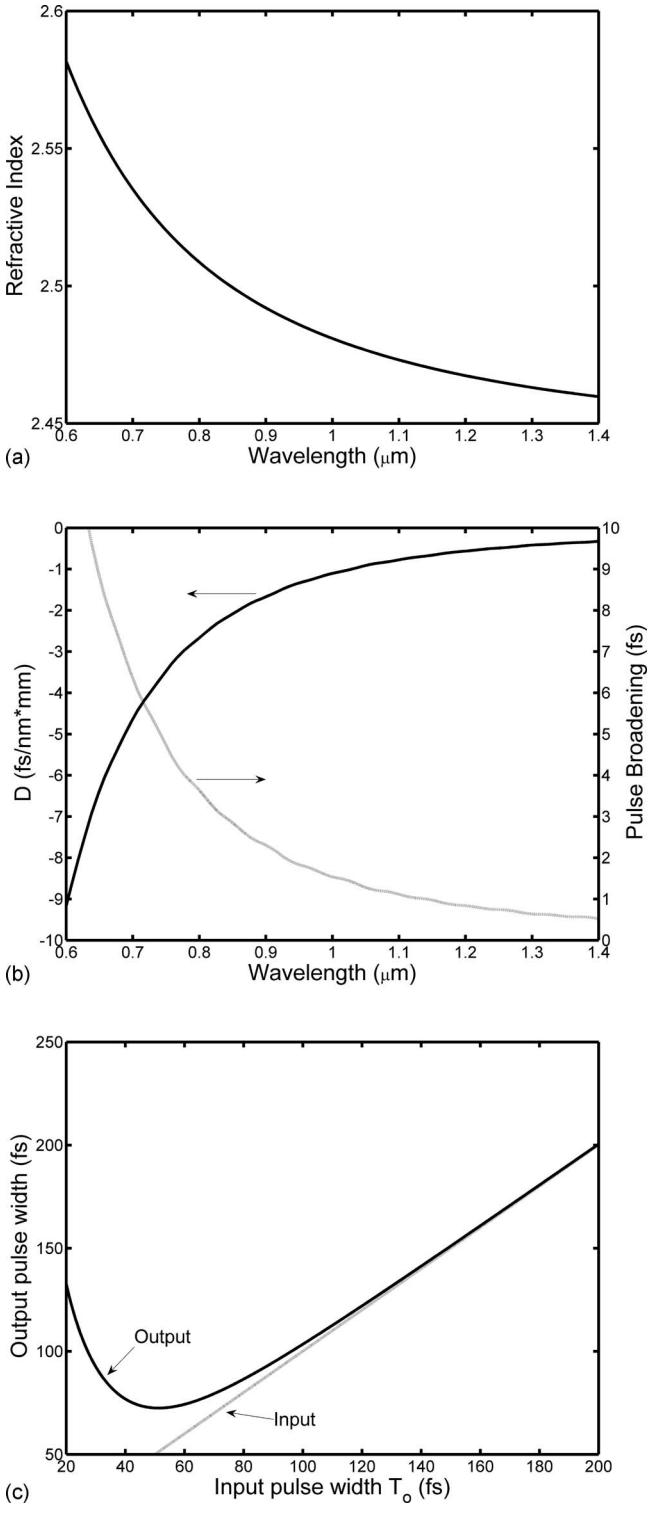

FIG. 2. (a) Measured refractive index, (b) calculated dispersion parameter D and the broadening of a 100 fs pulse, and (c) calculated output vs input pulse widths.

approximation, if only chromatic dispersion is considered and the optical pulse is Gaussian then the pulse width at the output can be calculated analytically as[7]

$$T(L) = \sqrt{T_0^2 + \left(\frac{\lambda^2 D}{2\pi c}\frac{L}{T_0}\right)^2}, \quad (1)$$

where T_0 is the input pulse width and L is the material thickness.

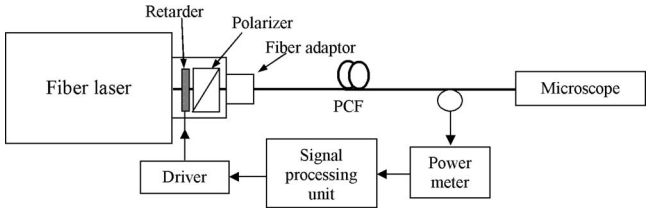

FIG. 3. Block diagram of wavelength control of femtosecond optical pulses using PCF and an electrically controlled polarization retarder.

The effect of pulse broadening depends both on the material dispersion and the spectral width of the input optical pulse. Assuming a 100 fs optical pulse at the modulator input, the pulse broadening is calculated by Eq. (1) and shown as the dashed line in Fig. 2(b). For signal wavelengths larger than 800 nm, the pulse broadening is less than 3.5 fs. This verifies our measurements and indicates that the pulse broadening effect is indeed negligible for our application. However, since the net pulse broadening is inversely proportional to the input pulse width T_0, the output pulse width will not decrease anymore with $T_0 < 70$ fs, and the narrowest output pulse width is approximately 50 fs as shown in Fig. 2(c). This sets the theoretical performance limit for the device described in this paper.

III. DYNAMIC WAVELENGTH SWITCHING USING PHOTONIC CRYSTAL FIBER

In addition to the switching of optical power, another desired functionality of the femtosecond laser source is the ability to dynamically switch the emission wavelength. Ti:sapphire lasers can be made tunable, but the wavelength tuning is usually obtained through mechanical adjustment, which is generally slow. Wavelength tuning of femtosecond pulses via SSFS has been reported through nonlinear optical fibers.[8] In this case, the frequency shift varies quasilinearly with fiber input power, and therefore intensity modulation of the laser converts to a frequency modulation at the fiber output. As an application example, we demonstrate that dynamic wavelength switch of femtosecond optical pulses can be accomplished with the intensity modulator based on the PMN-PT polarization retarder.

The experimental setup is diagrammed in Fig. 3. The output from the 800 nm femtosecond fiber laser (Femtolite F-100, IMRA Corp.) was coupled into a 5 m photonic crystal fiber (PCF) through the intensity modulator discussed above. The PCF (NL-1.8–710, Thorlabs Inc., Newton, NJ) has a zero-dispersion wavelength of 710 nm and effective core diameter of 1.8 μm. For this fiber the dispersion and dispersion slope at 800 nm are 68 ps/nm km and 0.59 ps/nm^2 km, respectively, and at 1000 nm they are 148 ps/nm km and 0.25 ps/nm^2 km.

A 5 m span of PCF was connected to the intensity modulator via a focusing lens as illustrated in Fig. 3, creating the tunable wavelength system for two-photon fiber laser excitation (TP-FLEX). Because of the miniature size of the PNM-PT cell, we were able to assemble the polarization modulator with a polarizer and a fiber adapter into a small package (ϕ=3 cm, L=3 cm), which is directly attached at

This article is copyrighted as indicated in the article. Reuse of AIP content is subject to the terms at: http://scitationnew.aip.org/termsconditions. Downloaded to IP: 129.237.46.100 On: Tue, 16 Sep 2014 13:59:45

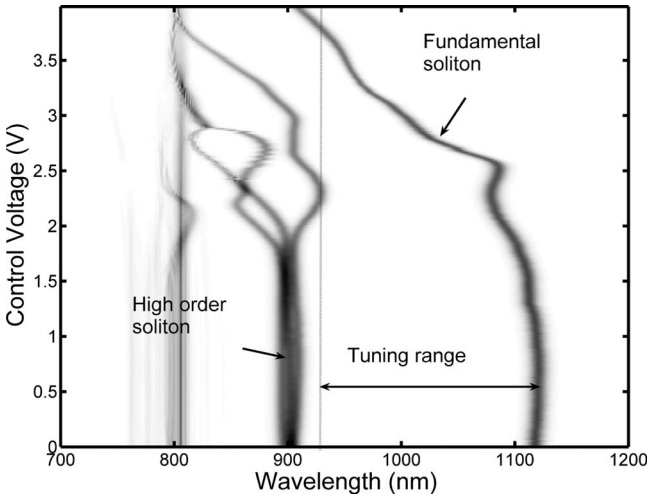

FIG. 4. Spectrogram measured with an optical spectrum analyzer, which shows both fundamental and high order solitons.

the fiber laser output. The wavelength shift is linear with power, and the intensity modulator has a square-law response to the applied bias voltage. Since the PCF produces a diverse spectrum along with leaky modes from the pump laser, some light always escapes through the side of the fiber in relation to the coupled power. By measuring this power level using a low speed photodetector attached to the side of the fiber coil, the actual optical signal power coupled into the PCF can be monitored. A feedback electronic signal-processing unit is designed, which can adjust the PNM-PT control voltage based on a predetermined calibration of power versus wavelength. This helps to stabilize the emission wavelength at the PCF output against fluctuations in laser pump power, temperature of the retarder, fiber alignment, and similar disturbances.

A spectrogram of the output versus applied signal voltage is shown in Fig. 4, with the color scale mapped to linear intensity. An electrical driver is used to linearly amplify the 0–5 V signal voltage into 0–300 V driving voltage on the polarization controller. Both the fundamental soliton and higher order solitons can be observed as the function of the signal voltage. The lowest applied voltage roughly corresponds to the highest optical transmission through the modulator and thus the largest soliton wavelength shift. With the wavelength of the femtosecond laser source at 800 nm, the fundamental soliton could be shifted as far as 1120 nm and beyond 1200 nm with more careful alignment. However, a second order soliton also exists at approximately 900 nm, which has to be filtered out in most practical applications. Therefore, a continuous wavelength tuning range of the TPFLEX system is greater than 200 nm without the need to change the long-pass filter.

We have measured the temporal pulse width of the input pump pulse and the output soliton pulses using an optical autocorrelator. The width of the pump pulse after the intensity modulator was roughly 111 fs, as shown in Fig. 5(a) with ten traces averaged and an estimated measurement error within ±5 fs. Figure 5(b) shows the autocorrelation of the fundamental soliton tuned to 1100 nm after propagation

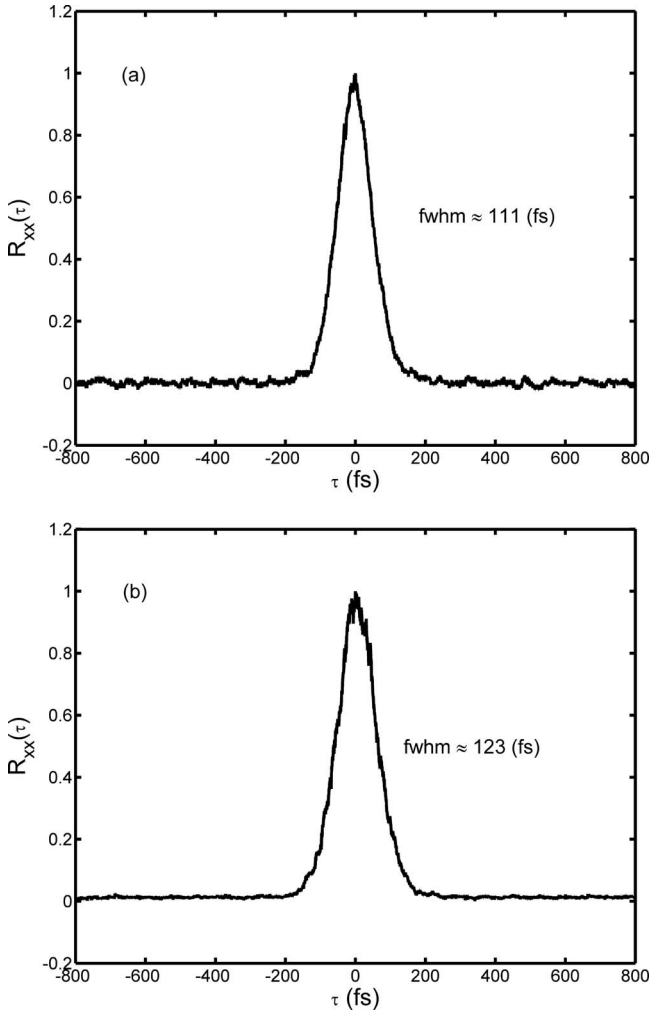

FIG. 5. Measured pulse width before (a) and after the nonlinear fiber (b).

through the 5 m PCF. The pulse width was approximately 123 fs, which is slightly larger than the pulse width at the input.

A scatter plot in Fig. 6 shows the relationship between the temporal pulse width and the spectral width for various

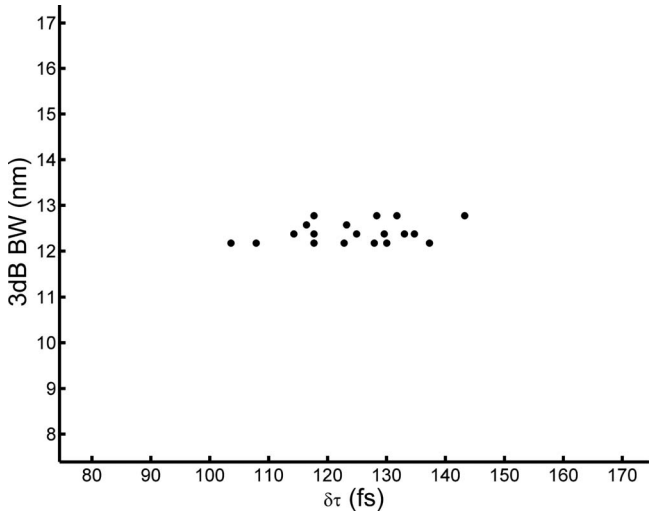

FIG. 6. Relationship between the temporal pulse width and the spectral width when the pulse wavelength was swept between 900 and 1100 nm.

This article is copyrighted as indicated in the article. Reuse of AIP content is subject to the terms at: http://scitationnew.aip.org/termsconditions. Downloaded to IP: 129.237.46.100 On: Tue, 16 Sep 2014 13:59:45

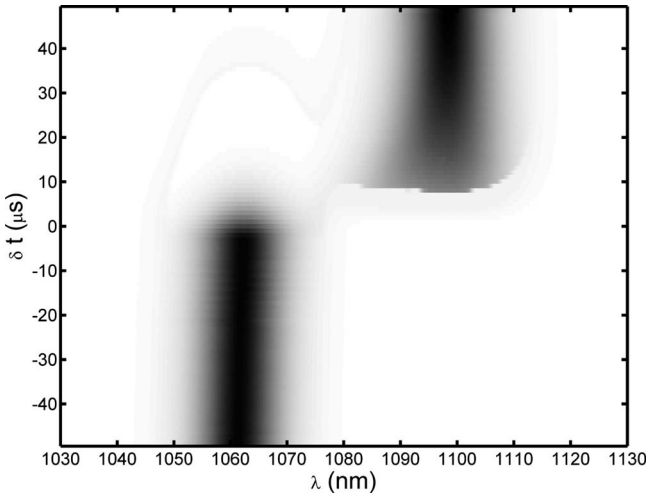

FIG. 7. Illustration of fast wavelength switch between 1060 and 1100 nm.

fundamental soliton wavelengths between 900 and 1100 nm. The time-bandwidth products, ranging from 0.375 to 0.45, are very close to the transform limit and therefore the phase distortion and frequency chirp are not significant concerns in this system.

In principle, the speed of wavelength switch in the PCF using the SSFS is limited only by the pulse propagation time in the fiber, which is approximately 25 ns if the fiber length is 5 m. In practice, this switch time is limited by the speed of the intensity modulator. In order to investigate the characteristic of dynamic wavelength switch of this system, we applied a 1 kHz square-wave modulation to switch between two preset wavelengths. Figure 7 shows the measured pulse spectrum (horizontal axis) as a function of time (vertical axis), using the triggered sampling mode of the optical spectrum analyzer (Ando AQ6317B). It is evident from Fig. 7 that the pulse wavelength was switched from 1060 to 1100 nm in less than 5 μs. In fact, since the capacitance of the ceramic polarization retarder is only about 680 pF, the switching speed is only limited by the power of the electrical driver. Currently, the driver we are using has 3 μs rise/fall time, which can be further improved if there is a need.

Because of the use of the triggered sampling mode, the measurement time is proportional to the total wavelength span of the optical spectrum analyzer. To avoid the unnecessarily long measurement time, we only used a relatively narrow wavelength span. The individual spectra of the image in Fig. 7 were measured in sequence over a roughly 30 min interval, while the wavelength was kept stable using power feedback control. This demonstrated high wavelength stability with less than 5 nm drift per hour. Any remaining deviation may be attributed to changing polarization state as the soliton travels throughout the fiber due to gradual motion or temperature fluctuation. Since our fiber is not a PM type, it may have slight rotational asymmetry and birefringence. This effect, while slight, may also be reduced using polarization maintaining fibers.

IV. SUMMARY

We have demonstrated an intensity modulator for 800 nm femtosecond pulses in near-IR wavelength window using a PMN-PT based optoceramic polarization retarder. Compared to both KDP-based pockels cells and acousto-optic modulators, this technique provides a simple, low cost, and reliable solution, which is miniature in size with low transmission loss. We demonstrated a practical application of this modulation method by creating a tunable wavelength femtosecond pulse source using a nonlinear PCF and the effect of the SSFS. With this system we achieved precise wavelength tuning over a 200 nm range suitable for two-photon imaging of biological materials. The system maintained high wavelength stability and achieved wavelength switching times of less than 5 μs. This switch speed may not be as fast as some other techniques, such as using $LiNbO_3$ and AOM;[4] it is fast enough for many biochemical applications such as multiphoton imaging, fluorescence resonance energy transfer (FRET), and fluorescence correlation spectroscopy (FCS). This switch speed is currently limited by the electrical driving circuit, which can be further improved in the future.

ACKNOWLEDGMENTS

This work was supported by the National Institute of Health under (Grant No. NIH-RR023142).

[1] W. Denk, J. H. Strickler, and W. W. Webb, Science **248**, 73 (1990).
[2] J. R. Unruh, E. S. Price, R. G. Molla, L. Stehno-Bittel, C. K. Johnson, and R. Hui, Opt. Express **14**, 9825 (2006).
[3] H. B. Sun and S. Kawata, J. Lightwave Technol. **21**, 624 (2003).
[4] S. Zeng, K. Bi, S. Xue, Y. Liu, X. Lv, and Q. Luo, Rev. Sci. Instrum. **78**, 015103 2007.
[5] H. Jiang, Y. K. Zou, Q. Chen, K. K. Li, R. Zhang, Y. Wang, H. Ming, and Z. Zheng, Proc. SPIE **5644**, 380 (2005).
[6] K. Li and Q. Wang, U.S. Patent No. 6,746,618 (8 June 2004).
[7] G. P. Agrawal, *Nonlinear Fiber Optics*, 3rd ed. (Academic, New York, 2001).
[8] N. Nishizawa and T. Goto, IEEE J. Sel. Top. Quantum Electron. **7**, 518 (2001).

This article is copyrighted as indicated in the article. Reuse of AIP content is subject to the terms at: http://scitationnew.aip.org/termsconditions. Downloaded to IP: 129.237.46.100 On: Tue, 16 Sep 2014 13:59:45